ISET Journal of Earthquake Technology, Paper No. 393, Vol. 36, No. 2-4, June-Dec. 1999, pp. 85-106

WAVELET TRANSFORM OF GROUND MOTIONS RECORDED AT TWO SITES DURING LOMA PRIETA EARTHQUAKE

Carlos E. Ventura and Mahmoud Rezai
Civil Engineering Department,
The University of British Columbia,
2324 Main Mall, Vancouver, BC, Canada V6T 1Z4

ABSTRACT

This paper explores the applicability of wavelet transform for the analysis of ground motion accelerations recorded on rock at Yerba Buena Island and on dredged sandfill at nearby Treasure Island about 2 km away during the 1989 Loma Prieta Earthquake in California. An interpretation of the results from this analysis is presented and discussed. The major important feature of this data set is that liquefaction occurred at the Treasure Island site during the earthquake. The Daubechies 20-coefficient and Haar Wavelet Transforms are utilized in this study. Results of the application of the wavelet transforms can be summarized as follows: most of the energy of the earthquake at the Treasure Island site is in the frequency range 0.58 - 1.77 Hz and arrives in the time interval between 11 and 15 seconds. For the Yerba Buena Island site, most of the energy lies within the frequency range 1.15 - 3.53 Hz and arrives between 8 to 13 seconds. The analysis indicates that there are some large peaks at the highest resolution in the wavelet transforms at the Treasure Island site which can be attributed to a progressive change in the stiffness characteristics of soil.

KEYWORDS: Wavelet Transform, Short-Time Fourier Transform, Joint Time-Frequency Analysis, Site Response, Liquefaction

INTRODUCTION

Ground motions generated by the 1989 California Loma Prieta Earthquake were recorded at two stations located in the San Francisco Bay, between San Francisco and Oakland, California (Shakal et al., 1989). One station is located in Yerba Buena Island while the other station is about 2 km away in Treasure Island. Treasure Island is a 400 acre land constructed in 1936-37 for activities celebrating the construction of the Golden Gate and San Francisco-Oakland Bay bridges. It is a man-made island constructed on loose, dredged sandfill underlain by soft bay mud and other recent and older sediments resting on bedrock. The structure of Treasure Island is essentially an upstream constructed hydraulic fill with a perimeter rock dike acting as a retaining system for the sands that were pumped or placed inside. The Yerba Buena Island is, however, a rock outcrop. The strong motion accelerometers at each station recorded ground motions in the N-S, E-W and up-down directions. The strongest components were in the E-W direction in which peak accelerations were 0.16g at Treasure Island and 0.06g at Yerba Buena Island. In the N-S direction the peak accelerations were 0.11g at Treasure Island and 0.03g at Yerba Buena Island. A notable amplification factor for surface motions recorded at the Treasure Island site relative to the rock motions at nearby Yerba Buena Island can be identified from the peak ground accelerations. The strong motions recorded at these two stations represent a pair of recordings at nearly the same location and distance from the fault rupture but with considerably different behaviour due to the effects of local geological conditions. Evidence of soil liquefaction on the Treasure Island site with numerous large sand boils was reported (Finn et al., 1993).

The emphasis of this paper is on the application of the wavelet transform for the analysis of accelerograms recorded during earthquakes. The wavelet transform is a relatively new method of signal analysis that has been gaining widespread use, especially for the analysis of signals with abrupt changes (Newland, 1993; Rezai and Ventura, 1995). The literature on wavelet transform is extensive, but most of it is devoted to processing of images or electronic and speech signals (Mallat, 1989; Kronland-Martinet et al., 1987). The wavelet transform basis functions are complex functions of the same shape that are concentrated in time and frequency. They are ideal to identify any phases of a signal with different frequency content and with localized time distribution.

We will explain the fundamentals of the wavelet transform in a manner suitable for an analyst who is familiar with the Fourier theory. We start with a review of the Fourier transform from which we give reasons for the use of the wavelet transform and its applications. Then, the application of the wavelet transform to the accelerograms recorded at Treasure and Yerba Buena Islands during the 1989 Loma Prieta earthquake is studied in order to demonstrate the potential of wavelet transform to analyse this type of strong motion data.

FOURIER TRANSFORM (FT)

The use of the FT concept reflects the philosophy that some aspects of a signal are most conveniently represented in time domain, whereas there are certain other aspects that are best represented in terms of its frequency content. The Discrete Fourier Transform (DFT) of a real time function $f(t)$ uniformly discretized at N points can be defined by:

$$F(k\Delta\omega) = \Delta t \sum_{n=0}^{N-1} f(n\Delta t) e^{-i(k\Delta\omega)(n\Delta t)} \tag{1}$$

in which $F(k\Delta\omega)$ are the values of the DFT at the discrete frequencies $k\Delta\omega$ and $i = \sqrt{-1}$. Δt is the time increment used to discretize the function. $f(n\Delta t)$ is a discrete sample of $f(t)$ evaluated at $t = n\Delta t$. $\Delta\omega = 1/N\Delta t$ is the frequency increment. n and k are integer numbers ranging from 0 to N-1.

The DFT is defined through a summation that covers the entire time duration of the function. Such transform can be readily applied to stationary signals whose properties do not change abruptly in time. However, if a signal contains sharp discontinuities (non-stationary signal), its Fourier representation requires a significant number of frequency components to capture these abrupt changes in time. This means that any localized discontinuity information is stretched out over the entire time axis as a single frequency component is always associated with an infinite time duration. As an example, if a function contains sudden transitions at some points, such as the one shown in Figure 1(a), we find that its DFT is composed of a number of peaks closely spaced at some particular frequencies, as shown in Figure 1(b). It is clear from Figure 1(b) that the predominant frequencies of 1 rad/s, 7 rad/s and 20 rad/s have been contaminated by the presence of other fictitious peak frequencies generated by the DFT. It is noted that a long temporal extension of the selected sinusoidal frequencies would significantly improve the prediction of DFT in terms of the predominant frequencies. It should be noted, however, that earthquake signals are random in nature and that the temporal extension of the recorded signals may change rapidly in time as a result of progressive damage throughout a structure or change in the stiffness characteristics of a medium. Therefore, in this example, the temporal extension of the signals was varied over relatively short time intervals to study the effect of FT on the signals that are not stationary. In this case, the DFT is not able to clearly identify what are the significant frequencies of the signal. Hence, the DFT cannot be efficiently applied to signals that have short temporal extension and contain sudden transitions at very short time intervals. Thus, alternate methods of data analysis need to be employed. One of these methods is the short-time Fourier transform, which is described in the following section.

SHORT-TIME FOURIER TRANSFORM (STFT)

In order to accommodate the sudden variations of frequency components of a function in short time intervals and to localize the information provided by the FT, the idea of STFT or window Fourier transform was introduced by Gabor (Gabor, 1946). The STFT looks at $f(t)$ through a window over which the function is approximately stationary. The window function is generally a real even function with the characteristics of a low-pass filter. The discrete window Fourier transform of a real discrete-time function $f(n\Delta t)$ is defined by:

$$F_{STFT}(k\Delta\omega, b) = \Delta t \sum_{n=0}^{N-1} f(n\Delta t) w(n\Delta t - b) e^{-i(k\Delta\omega)(n\Delta t)} \tag{2}$$

where b is the time shifting parameter and $w(n\Delta t)$ is the window function. Other terms were defined above.

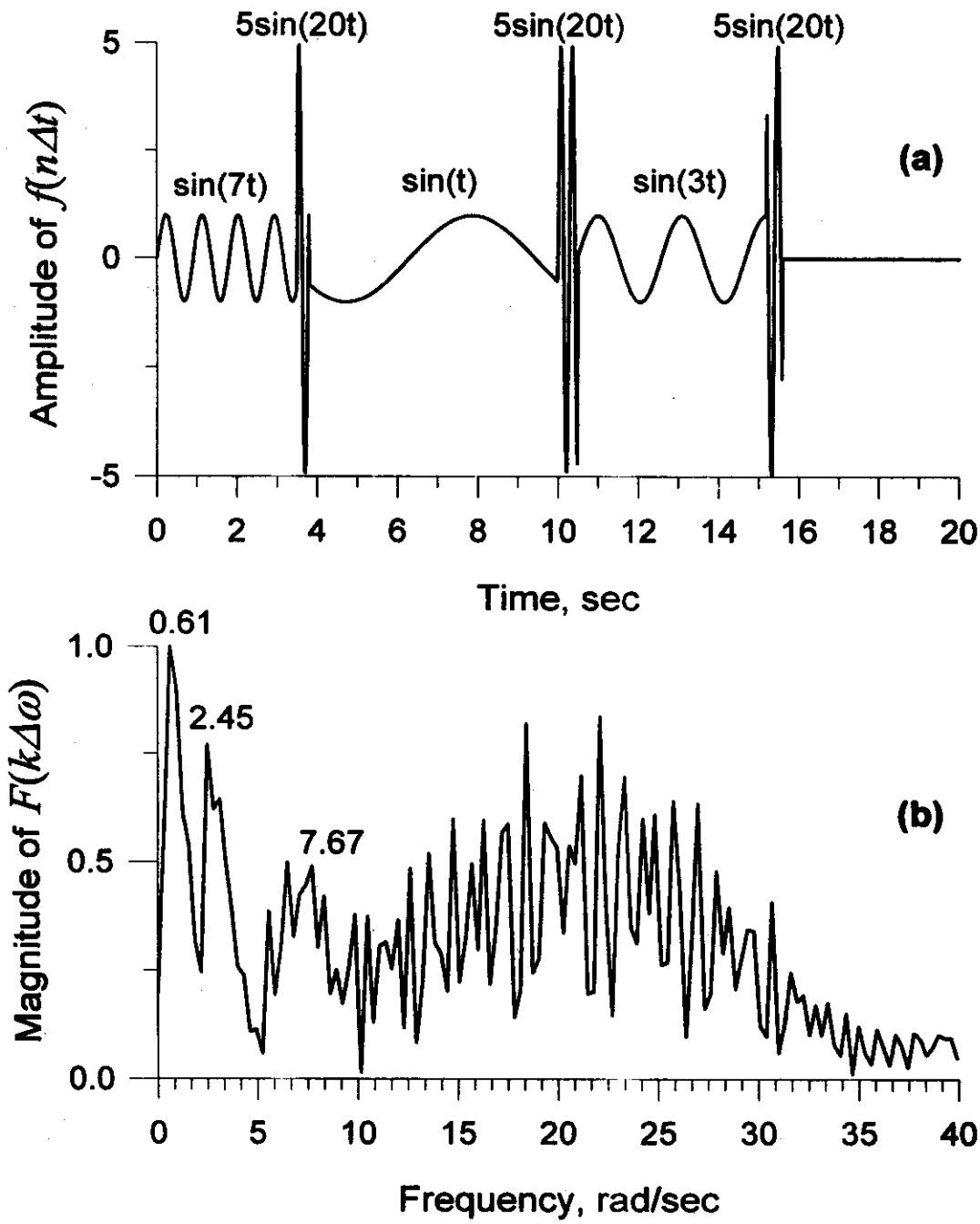

Fig. 1 (a) Example of a signal $f(n\Delta t)$ with sharp discontinuities,
(b) Magnitude of FT of the signal, $F(k\Delta\omega)$

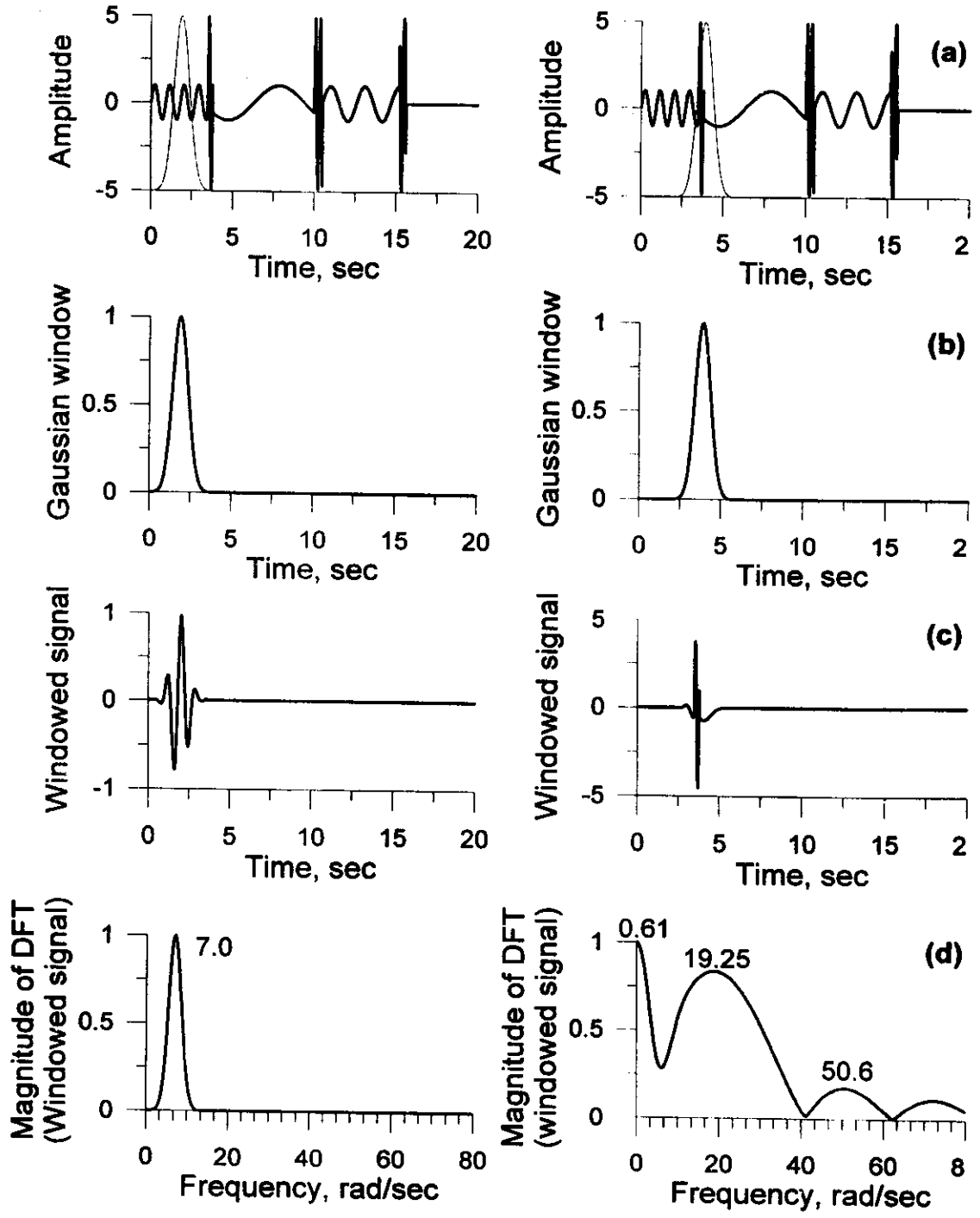

Fig. 2 STFT of a signal with sharp discontinuities (a) signal in time domain, (b) location of the window function, (c) windowed signal, (d) magnitude of FT of the windowed signal

The operation indicated by Equation (2) results in a separate Fourier transform for each part of the function conforming to each location b of the center of the window. The transform is now time-dependent (based on where the window function is located) and thus establishes a time-frequency description of $f(n\Delta t)$.

A drawback of the STFT is that the bandwidth of the window function is fixed, which means that it cannot adapt to the characteristics of $f(n\Delta t)$ at different locations. For the case of a signal with high frequency components, many cycles are captured by the window. However, for a low frequency signal, very few cycles are within the window. This indicates that for a window of fixed bandwidth, the efficiency of the STFT improves at higher frequencies, and declines as the frequency content of $f(n\Delta t)$ decreases. Thus, it would be more desirable here to have a window whose width adjusts itself with frequency content of $f(n\Delta t)$.

The advantages and limitations of the STFT can be clearly appreciated when it is applied to the signal shown in Figure 1. The results of the STFT analysis for two selected window locations are shown in Figure 2. The purpose here is to demonstrate that if the length of the selected window lies within a part of the function that is stationary, it can thoroughly detect the dominant frequency of the signal at that particular window location. Here, we have selected the Gaussian window proposed by Gabor (1946), as shown in Figure 2(b). Gabor selected the Gaussian window because its FT is concentrated in the low frequencies and it has the same shape as that of $e^{i\omega t}$ of the function in the time domain. Other window functions used in practice are generalizations of the Gaussian window function with different frequency characteristics.

As the window is placed where there is no sudden transition in the frequency content of the selected signal, the STFT results in a single dominant peak at 7 rad/sec. However, if the window is placed where there is a sudden transition in the frequency content of the signal (e.g., transition from $\sin(7t)$ to $\sin(20t)$ and vice versa), the STFT like the FT generates a number of peaks that might not even exist in $f(n\Delta t)$, as shown in part (d) of Figure 2. Obviously, to overcome this problem, the length or location of the window must be adjusted accordingly. It should be noted that the STFT peaks are not concentrated at their corresponding dominant frequencies mainly because of the short length of the window and that the peaks were obtained for a single location of the window.

CONTINUOUS-TIME WAVELET TRANSFORM (CTWT)

In order to avoid the inconvenience of a transform having a fixed resolution in the spatial and frequency domains, Grossman and Morlet (1974) proposed a new type of signal decomposition based on dilations. The wavelet transform (WT) can be considered as a further modification of the STFT that allows nonuniform window functions. The WT can be used to represent a time domain function as a linear combination of a family of basis functions. All the basis functions are generated by scaling (dilation or contraction) and shifting of a single function, $\Psi(t)$, called mother wavelet. A family of wavelet bases, $\Psi_{a,b}(t)$, is given by:

$$\Psi_{a,b}(t) = \frac{1}{\sqrt{a}}\Psi\left(\frac{t-b}{a}\right) \tag{3}$$

where a is the scaling parameter and b is the shifting variable. The scaled wavelets, $\Psi_{a,b}(t)$, contain an energy normalization term, $1/\sqrt{a}$, that keeps the energy of the scaled wavelets the same as the energy in the original mother wavelet. Figure 3(a) shows a typical example of dilated versions of a special type of mother wavelet developed by Meyer (1986). Note the constant shape of these scaled functions and the same number of oscillations in each wavelet. The corresponding magnitude of the FT of each of the wavelets depicted in Figure 3(a) is shown in Figure 3(b). This figure shows that each scaled wavelet can be viewed as a bandpass filter with a particular frequency bandwidth and a centre frequency, f_0. It can be seen that this oscillating frequency, f_0 appears at the centre of the frequency band of the mother wavelet. The frequency bandwidth of each wavelet is a function of the scaling parameter a. For a small

value of a, a basis function becomes a stretched wavelet, corresponding to a low frequency function. For a large value of a, the basis function becomes a contracted version of the prototype wavelet, conforming to a high frequency function.

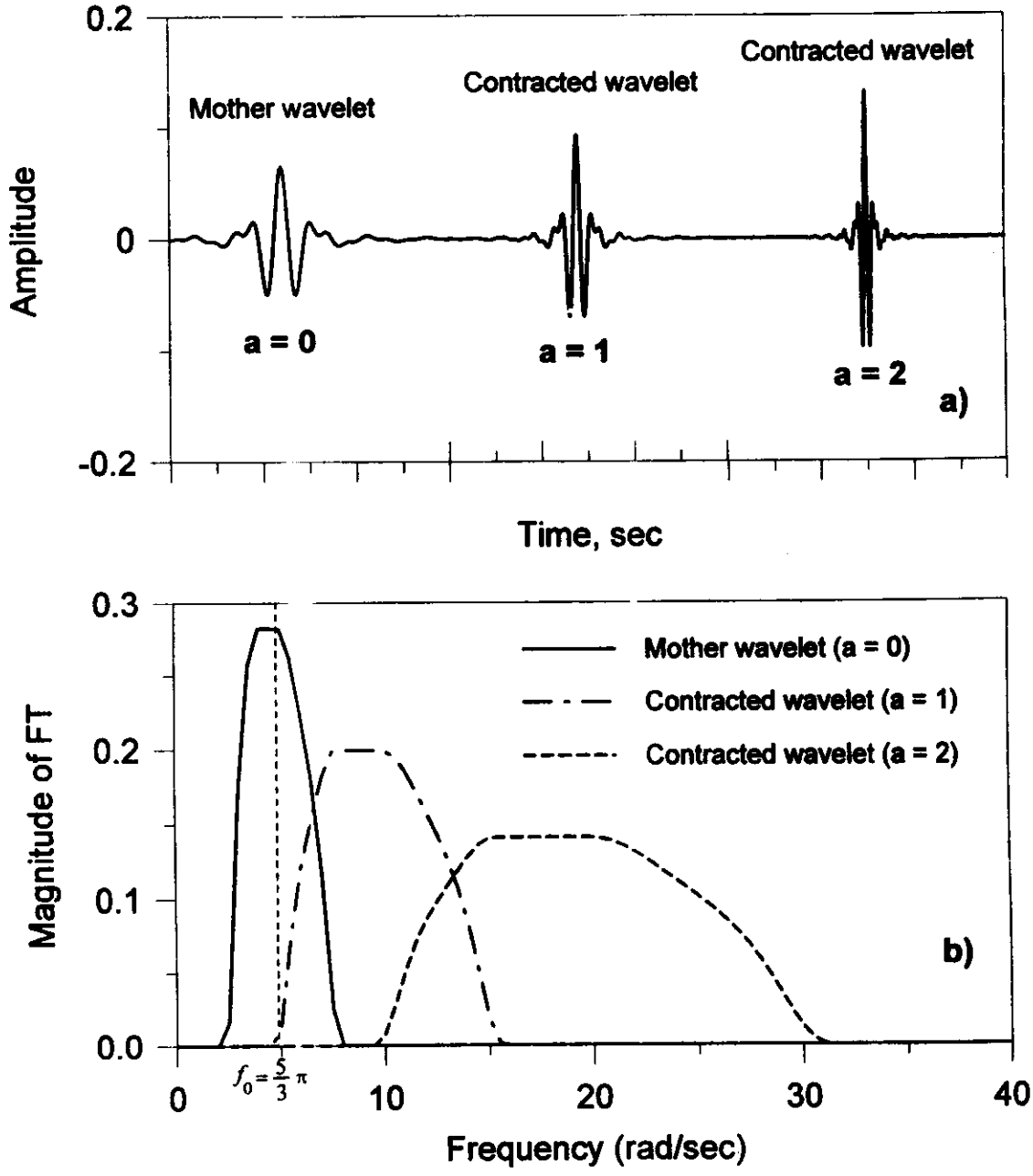

Fig. 3 (a) Example of Meyer's mother wavelet, $\Psi_{a,b}(t)$, and two contracted versions of it,
(b) Magnitude of FT of Meyer's wavelets shown above

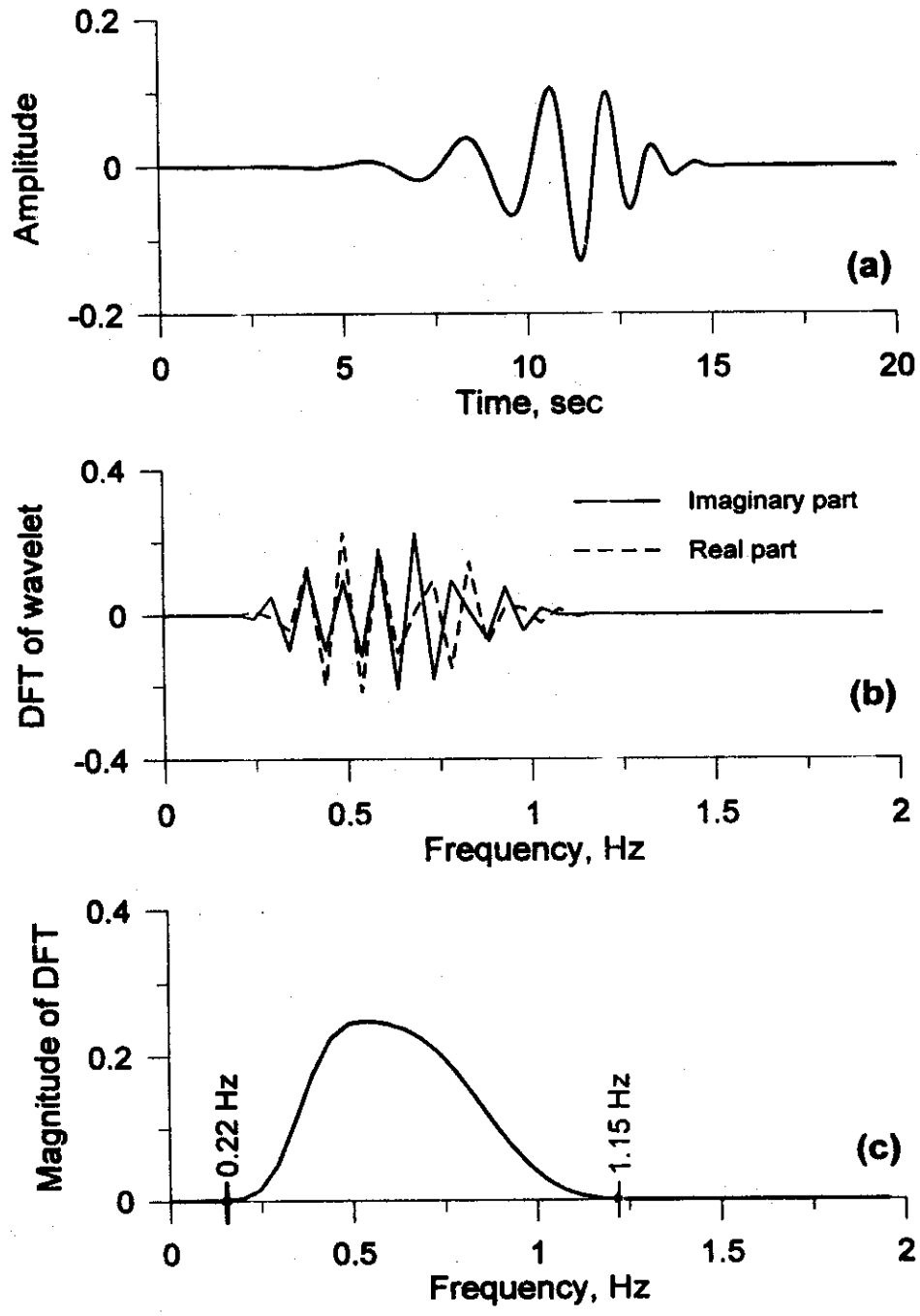

Fig. 4 Daubechies 20-coefficient wavelet (scale $p = 5$) and its FT (a) waveform in time domain, (b) FT real and imaginary parts, (c) magnitude in frequency domain

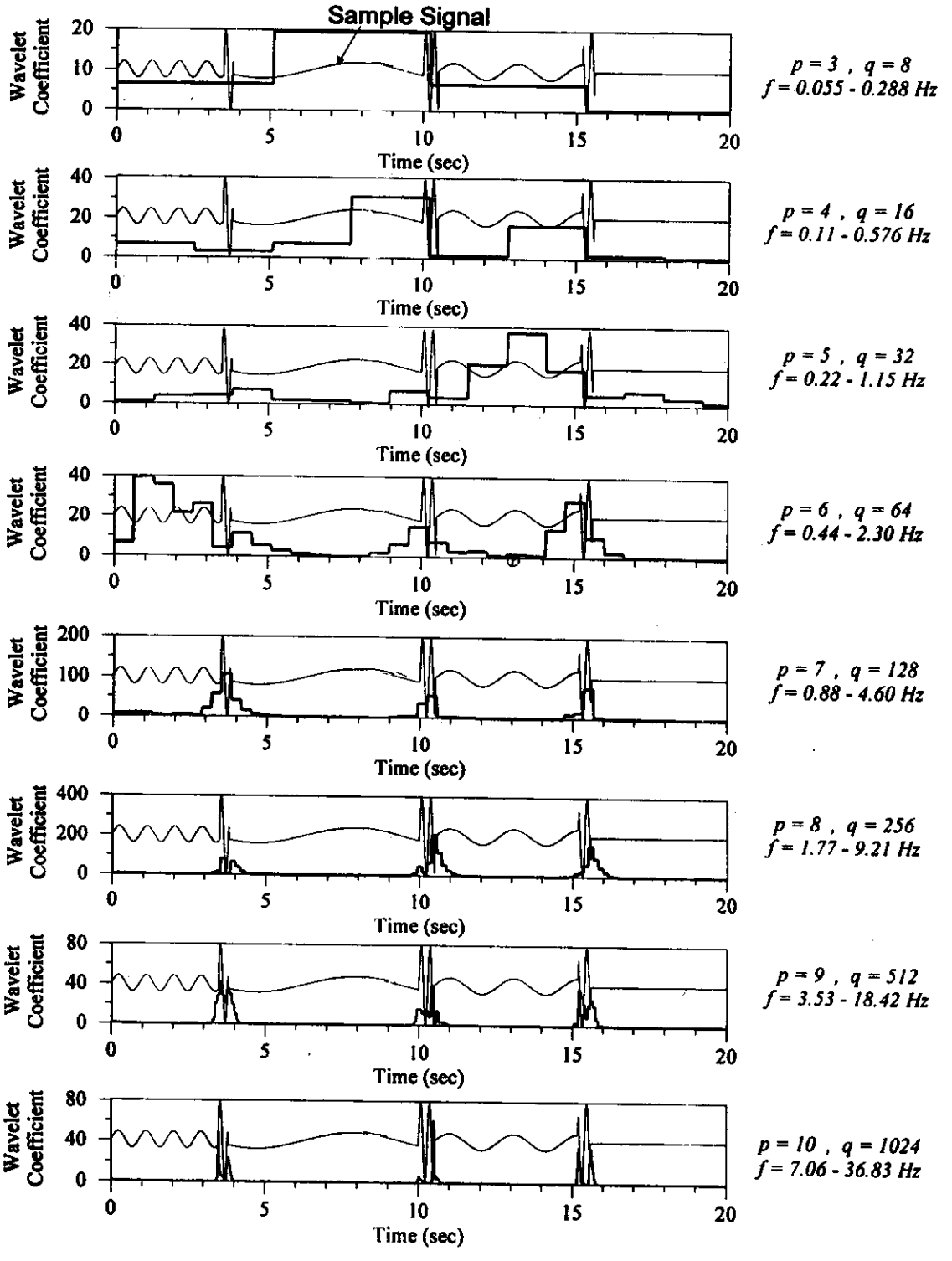

Fig. 5 Absolute magnitude of coefficients for the Daubechies 20-coefficient wavelet analysis of the sample signal, with bars at the center of the corresponding analyzing wavelet in time q for each frequency range p (thin line represents the sample signal for comparison purposes)

Similar to the STFT, the WT can provide the time-frequency characteristic of a signal. It can be utilized to reveal estimates of the frequency content of a signal for a particular time interval. It is a scale-invariant transform which is inherently able to deal with short duration features (local) and long duration features (global) of a signal. The CTWT of a time function $f(t)$, denoted as $W(a,b)$, is defined as the inner product of $f(t)$ and $\Psi_{a,b}(t)$:

$$W(a,b)=\frac{1}{\sqrt{a}}\int_{-\infty}^{+\infty} f(t)\Psi_{a,b}^{*}\left(\frac{t-b}{a}\right)dt \tag{4}$$

in which $\Psi_{a,b}^{*}(t)$ is the complex conjugate of $\Psi_{a,b}(t)$. The reconstruction formula is given as:

$$f(t)=\frac{1}{C_{\Psi}}\int_{-\infty}^{+\infty}\frac{da}{a^{2}}\int_{-\infty}^{+\infty}\frac{1}{\sqrt{a}}W(a,b)\Psi_{a,b}\left(\frac{t-b}{a}\right)db \tag{5}$$

In order to reconstruct $f(t)$ from its wavelet transform, C_{Ψ} must not be infinity. This requires that the FT of $\Psi(t)$, defined as $\Psi(\omega)$, must satisfy the admissibility condition:

$$C_{\Psi}=2\pi\int_{-\infty}^{+\infty}\frac{|\Psi(\omega)|^{2}}{\omega}d\omega<+\infty \tag{6}$$

The above admissibility condition is indeed satisfied whenever $\Psi(t)$ is of finite energy and has a mean value of zero. Additional details on the wavelet transform are presented by Rioul and Vetterli (1991) and Vetterli and Herley (1992).

DISCRETE WAVELET TRANSFORM (DWT)

For the DWT, it is possible to discretize the translation and dilation parameters of the continuous wavelet bases while still being able to perfectly reconstruct a function from its transform. Daubechies (1988) discretized the time-scale parameters a and b in the following way:

$$a=a_{0}^{p}\qquad b=qa_{0}^{p}T\qquad \text{where}\qquad a_{0}>1\ \text{and}\ T\neq 0 \tag{7}$$

in which p and q belong to the set of integer numbers Z, and T is the sampling period. The scale parameter a is set as integer power of a fixed parameter a_0.

The choice for T is arbitrary since the translation parameter b can be adjusted to fix any value of T. For convenience, T is set to one $(T=1)$. We see from this choice that the shift parameter, b, depends on the scale parameter a_0^p. If the scale, $1/\sqrt{a_0^p}$, is large, then the size of the translation parameter increases. This is intuitively correct since a large scale implies that details are not so important, and the scaled wavelet basis can be translated in larger steps.

DISCRETE-TIME WAVELET TRANSFORM (DTWT)

In most of practical applications, the function that we wish to transform is not continuous but discrete. Suitable selection of a_0 and f_0 can allow the wavelet series to cover all frequencies of interest. It may be suggested that a_0 and f_0 are chosen to let the central frequencies of the wavelets have octave band intervals. Let the scale discretization parameter a_0^p be selected as $a_0^p=2^p$, then the central frequencies of the wavelets are $f_0^p=a_0^p f_0$. The choice of $a_0=2$ for which $\Psi_{p,q}(t)$ constitutes an orthonormal basis, minimizes redundant information and permits an easy implementation for discrete data sets. Any arbitrary signal can then be represented exactly as a sum of basis functions weighted by the wavelet components. Since time dilation by a factor of 2 can be efficiently implemented simply by dropping every other sample of a discrete-time signal (sub-sampling by a factor of 2), the transform to be applied here (DTWT) only considers time scaling by powers of 2. An important particular case of the WT is that

some wavelets $\Psi_{p,q}(t)$ exist such that the family is an orthogonal basis (Chui, 1992 and Daubechies, 1992):

$$\Psi_{p,q}(t)=\frac{1}{\sqrt{2^p}}\Psi\left(2^{-p}t-q\right) \tag{8}$$

Orthogonal wavelets, such as the well-known Daubechies wavelet series, offer fast algorithms and no redundancy in the decomposition (Daubechies, 1992 and Newland, 1993).

In order to demonstrate the superiority of the WT over the conventional FT, the signal in Figure 1 is analysed using the Daubechies 20-coefficient mother wavelet (Daubechies, 1992). This wavelet is a smooth bandpass function and convenient for filtering a signal at different scales. It is band-limited in frequency for each scaling parameter p. The frequency bandwidth of $\Psi_{p,q}(\omega)$ depends on the scaling parameter p and is bounded by $2^p/72.5 \le f \le 2^p/13.9$ where f is given in Hz. Figure 4 shows time and frequency plots of the Daubechies 20-coefficient wavelet. Note that this wavelet at the level shown $(p=5)$ is band-limited between $0.22 \le f \le 1.15$ Hz. Other levels would give wavelets with the same shape but different scales, positions and frequency content.

Figure 5 demonstrates the WT coefficients of the signal in Figure 1 at 8 different scales. In this figure, each step is a representation of one shift for the analysing wavelet and the corresponding wavelet component for that particular time location. For example, with $p=5$, there are $q=2^5=32$ components (one component for each shift) or steps. Because of multiple scaling capability, the WT is able to detect all the frequency components of the signal at different scales (the corresponding frequency band for each wavelet basis is shown on the right side of the figure). Comparing with the STFT where only one resolution is used for describing the smail and large size of the features, the WT distribution gives multiple resolution so that different sizes of details in the analysed signal have been described effectively from low to high scales.

Since the Daubechies 20-coefficient wavelet is band-limited in frequency, wavelets with a larger scaling factor p capture the higher frequency components of the signal. The largest value of p will provide us with the exact locations of the sudden frequency transition points in the signal. These transition points are captured at the start and the end of $\sin(20t)$ waveform, where there is an abrupt change in the frequency content of the signal.

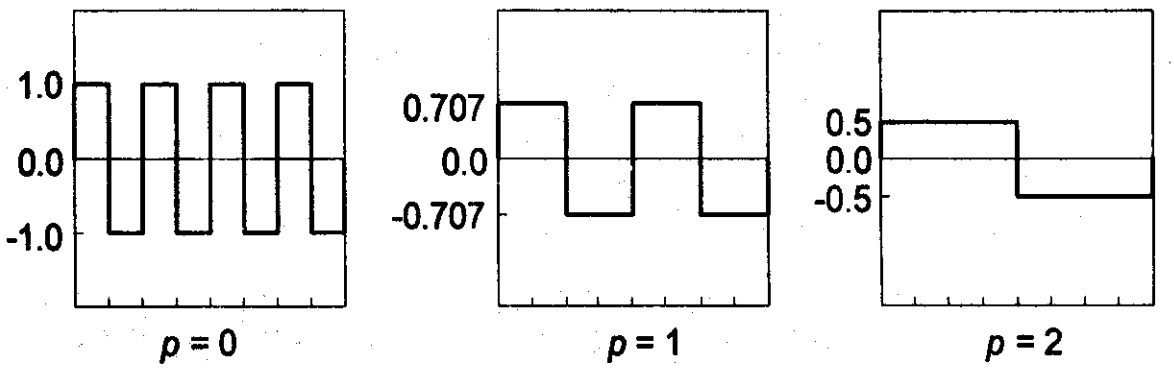

Fig. 6 Haar wavelet bases at three different scales

In the present study, we used two different sets of discrete orthonormal wavelets: Daubechies 20-coefficient wavelet (Daubechies, 1992) and Haar wavelet (Strang, 1989). The analysing Daubechies 20-coefficient wavelet was discussed in the preceding paragraphs. The Haar wavelet is a compact unsmooth function which is better for lower accuracy approximation and for signals with sharp discontinuities. Figure 6 shows the time domain representation of Haar basis wavelet at three different scales. We used

the above wavelets to analyse the strong motion data recorded at Yerba Buena Island and nearby Treasure Island during the Loma Prieta earthquake in 1989.

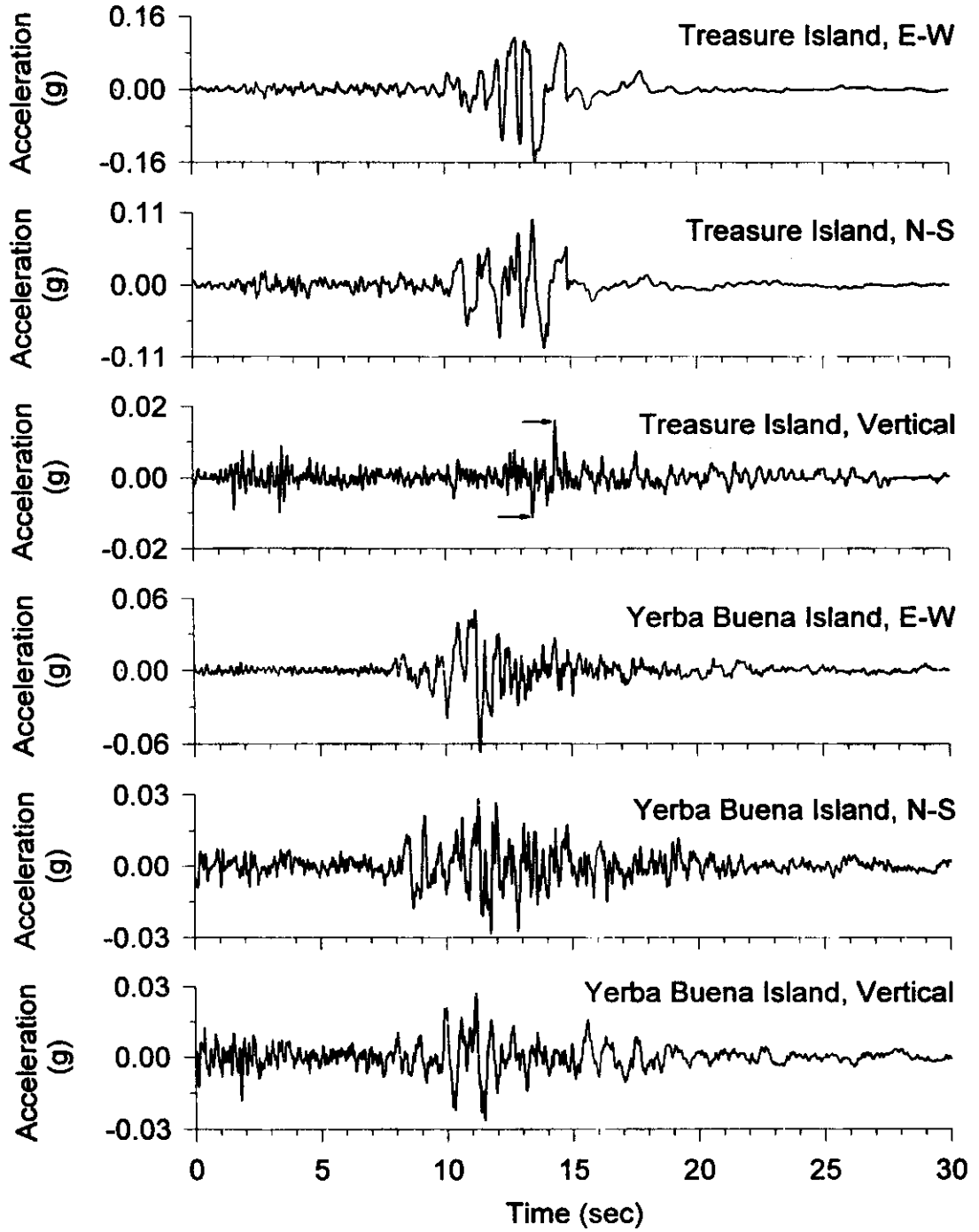

Fig. 7 Components of acceleration records at Treasure and Yerba Buena Islands during 1989 Loma Prieta Earthquake

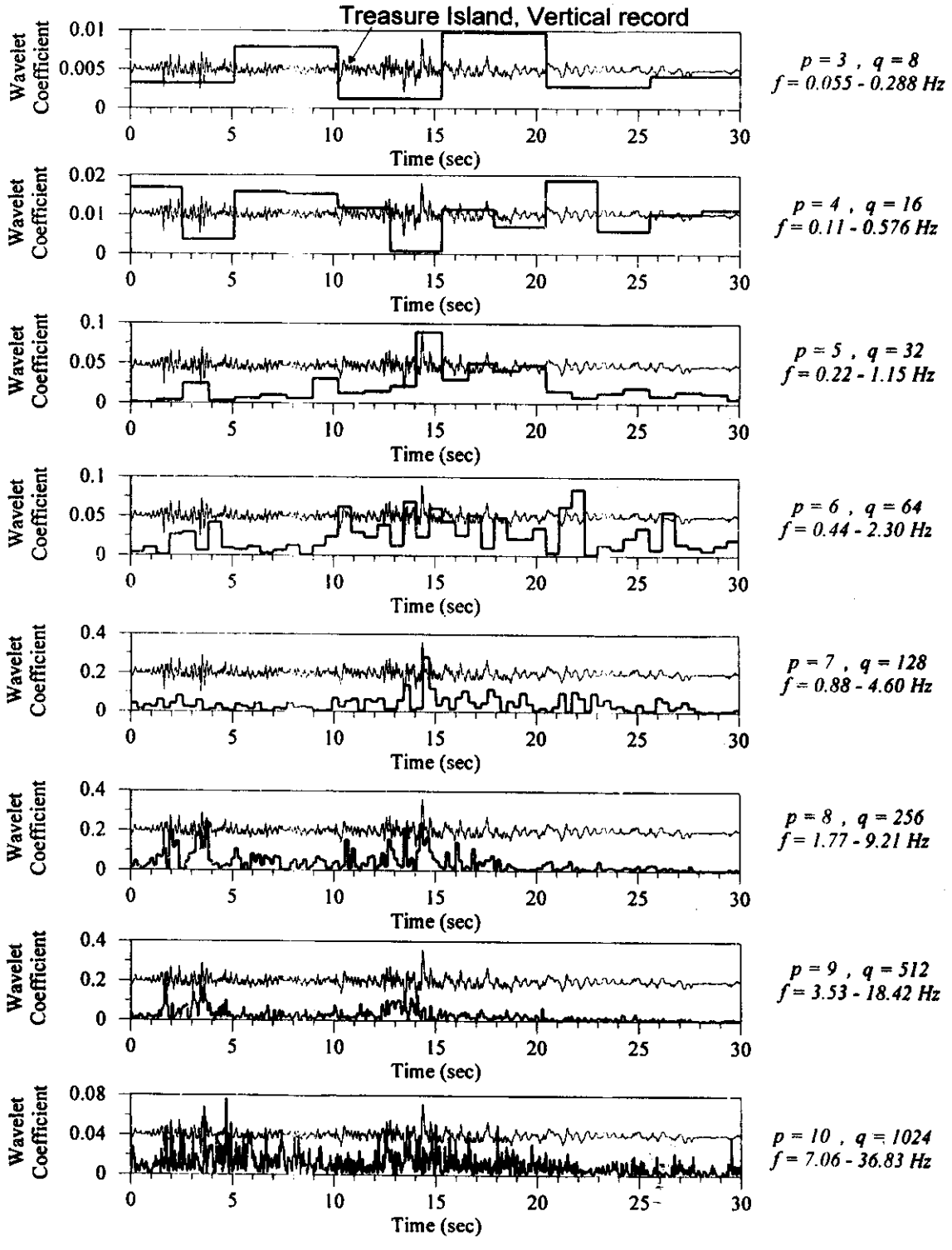

Fig. 8 Absolute magnitude of coefficients for the Daubechies 20-coefficient wavelet analysis of the Treasure Island vertical acceleration, with bars at the center of the corresponding analyzing wavelet in time q for each frequency range p (thin line represents the recorded vertical acceleration for comparison purposes)

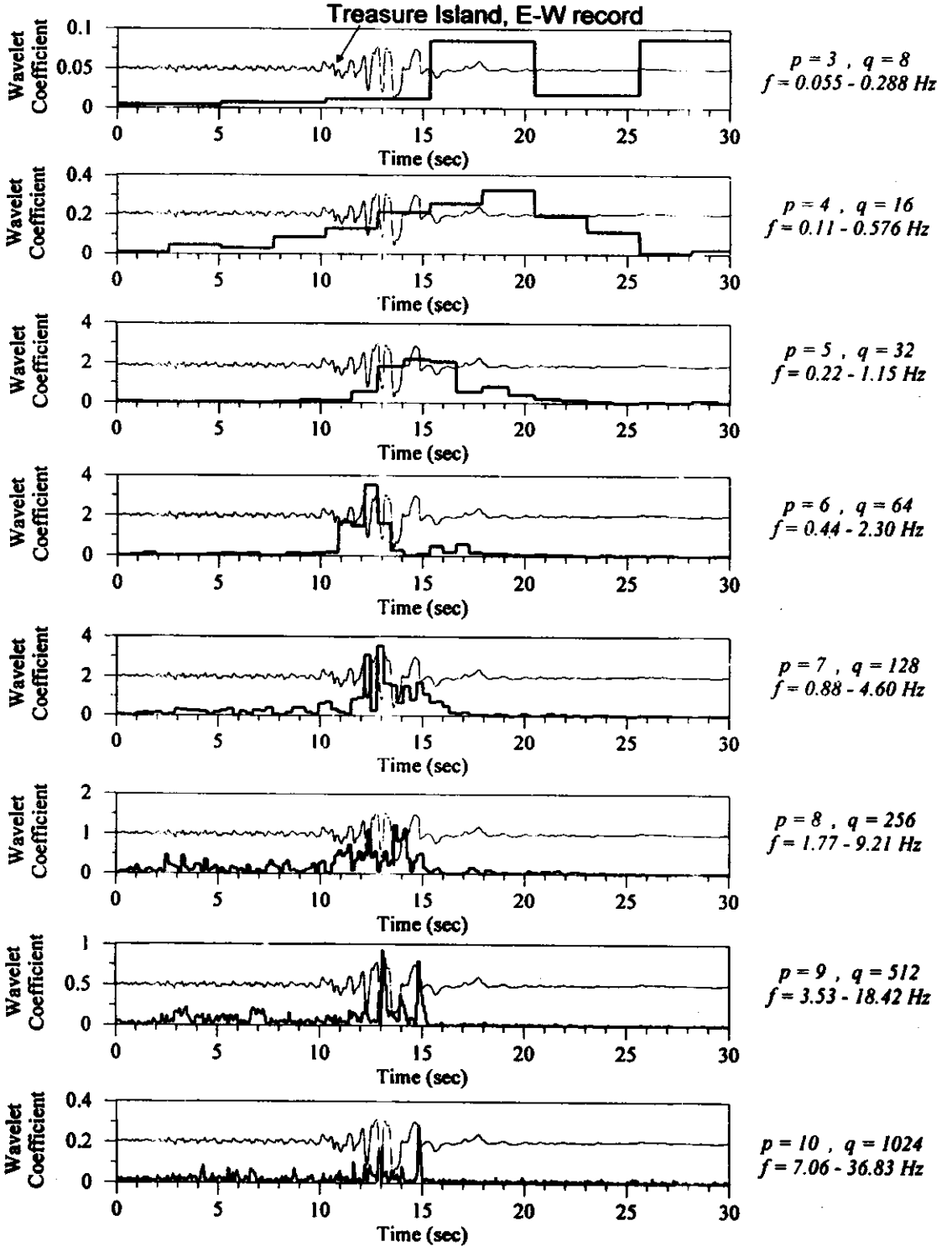

Fig. 9 Absolute magnitude of coefficients for the Daubechies 20-coefficient wavelet analysis of the Treasure Island E-W acceleration, with bars at the center of the corresponding analyzing wavelet in time q for each frequency range p (thin line represents the recorded E-W acceleration for comparison purposes)

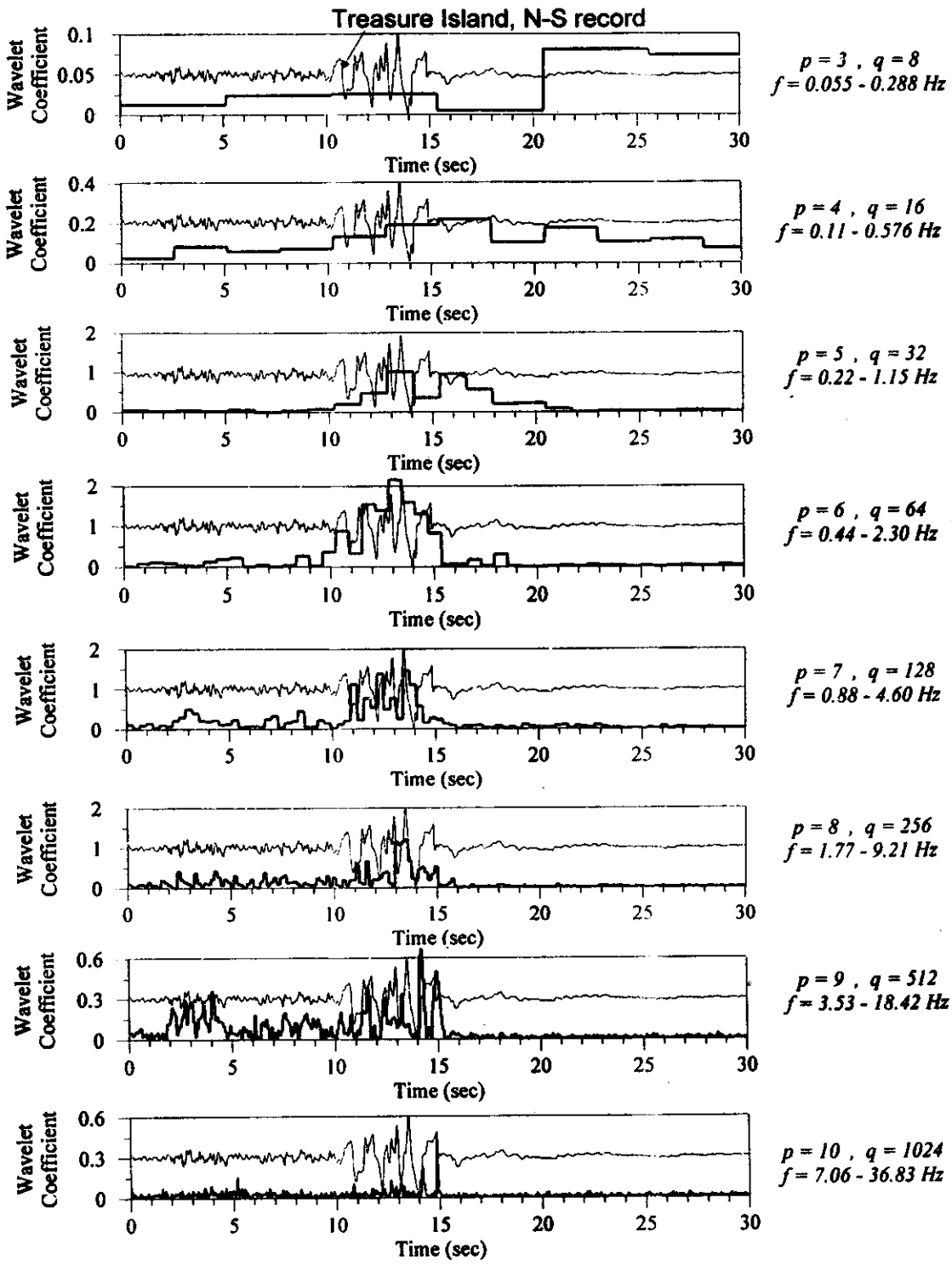

Fig. 10 Absolute magnitude of coefficients for the Daubechies 20-coefficient wavelet analysis of the Treasure Island N-S acceleration, with bars at the center of the corresponding analyzing wavelet in time q for each frequency range p (thin line represents the recorded N-S acceleration for comparison purposes)

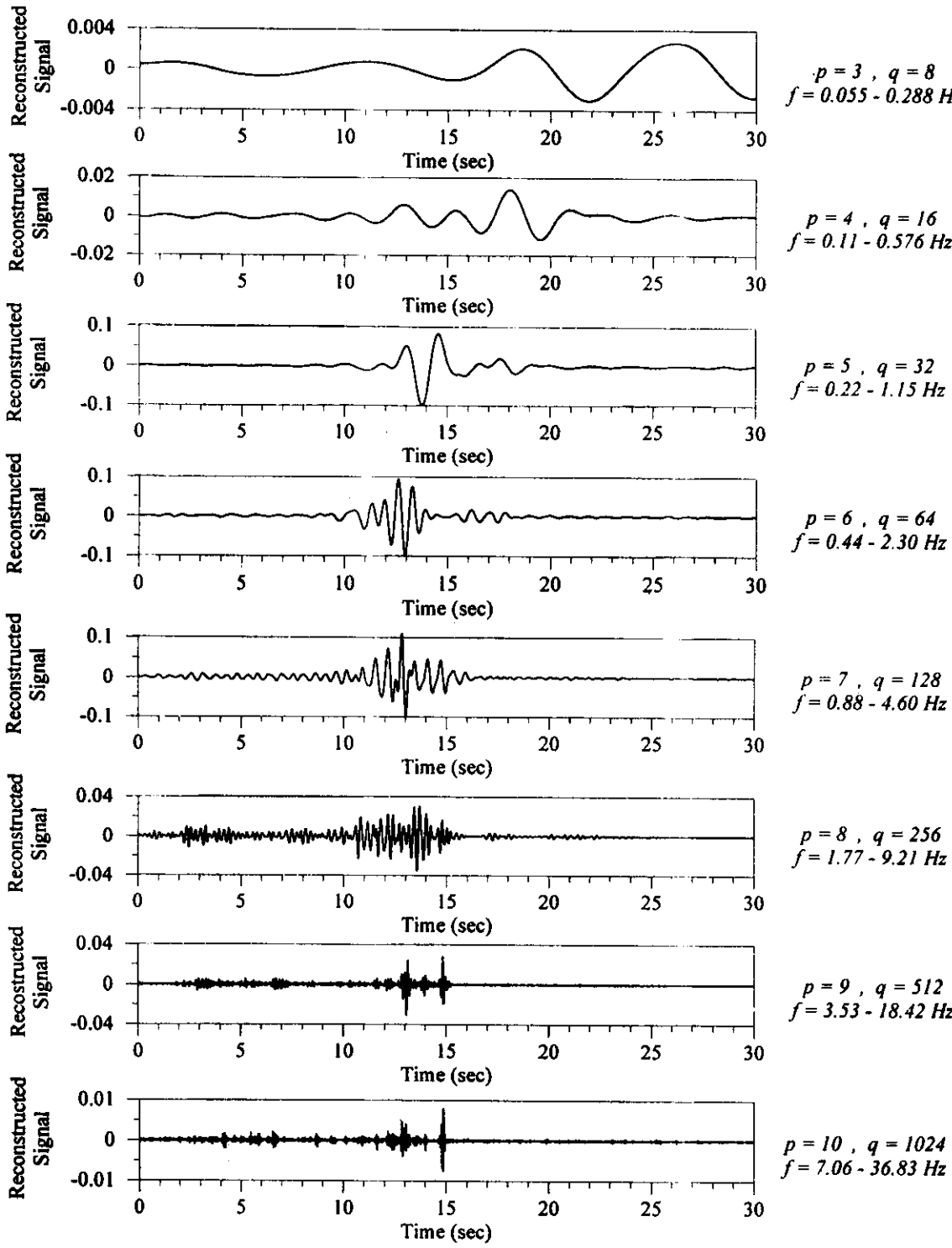

Fig. 11 Time-domain representation of analyzing wavelets for each p for E-W acceleration at Treasure Island (these plots may be interpreted as band-passed accelerations for the corresponding frequency range for each p)

ANALYSIS OF STRONG GROUND MOTION DATA

An important application of recordings of free field strong motion accelerograms from severe earthquakes is the analysis of the response of the upper few hundred meters of the earth to waves from these earthquakes. It is well known that surface geologic characteristics can significantly affect the nature of strong ground shaking collected at each location. In this case, evidence of soil liquefaction was widespread on the interior of the Treasure Island with numerous large sand boils following Loma Prieta earthquake. Figure 7 shows the E-W, N-S and vertical components of acceleration data recorded at Treasure and Yerba Buena Islands during the main shock event. The effect of soil conditions on the intensity and characteristics of the ground motion recordings at the two sites is evident from the recorded accelerograms. The duration of severe strong shaking lasted approximately 5 to 7 seconds for the horizontal excitation. The main horizontal motions were in the time range of 10 to 15 seconds for Treasure Island and 8 to 15 seconds for Yerba Buena Island, then decaying rapidly in time. The E-W accelerations have larger amplitudes compared to the N-S accelerations mainly because of the direction of fault rupture. The vertical acceleration was about 10% of the E-W acceleration for the Treasure Island and about 40% of the corresponding E-W acceleration for the Yerba Buena Island. The Treasure Island record was amplified, as the soil conditions there are different than the bedrock characteristics of the Yerba Buena Island.

We can easily recognize the anomalous behaviour of the Treasure Island site between 13 and 15 seconds in the E-W and N-S records. This part of the records seems to be dominated by waves of longer period compared to the main part. The vertical record at Treasure Island site shows two bursts between 13 and 15 seconds, as shown by the arrows in Figure 6. These anomalous pulses may indicate some specific characteristics of the soil evolved during that particular time period. The impulse-like phase between $t = 14$ seconds and $t = 15$ seconds shows a large late energy arrival at this time interval. Such a behaviour is not identified in the Yerba Buena Island records. We therefore conclude that completely different signals in terms of amplitude and frequency content arrived at the two sites between 8 to 15 seconds.

WAVELET ANALYSIS AND RESULTS

Conventional Fourier analysis of the time domain accelerograms may not reveal the characteristics of the above-mentioned phenomena thoroughly. Since the events are apparently localized in both time and frequency, the WT analysis is expected to be suitable to identify the characteristics of the signals. We, therefore, conducted the wavelet analysis, using the Daubechies 20-coefficient analysing wavelet described in the previous section, of the acceleration data recorded at Treasure and Yerba Buena Islands. Figures 8, 9 and 10 show the results of the WT for the vertical, E-W and N-S components of Treasure Island acceleration, respectively. The above figures represent normalized values of wavelet coefficients $W_{p,q}\left(i.e.\sqrt{2^p}\,|W_{p,q}|\right)$ for different values of p (frequency scale). Each bar is then located at the time of the centre of an analysing wavelet for each q (time scale). Since the Daubechies 20-coefficient wavelet is band-limited in frequency, wavelets with a larger p cover the higher frequency content. Figure 11 shows the reconstructed E-W acceleration of Treasure Island only from wavelets of one value of p over all $q's$. In other words, these accelerations correspond to bandpassed accelerations although the concept of the WT is entirely different as explained in the previous sections.

As it is observed from the distribution of peak wavelet coefficients at different scales in Figure 8, the main energy of the vertical motion at Treasure Island site lies in the frequency range of $p = 7$ to 9 or about 2.30-7.06 Hz. The wavelet amplitudes in this frequency range decay after 15 seconds and no significant later arrivals are observed. It is noted that for $p = 10$ or $7.06 < f < 36.83$ Hz and $p = 6$ or $0.88 < f < 2.30$ Hz, the normalized wavelet coefficients are relatively small indicating that little energy was concentrated in the frequency range below 2.30 Hz and above 7.06 Hz. The two anomalous phases indicated by arrows in Figure 7 are captured by the peak wavelet coefficients at scales $p = 7$ and 8. The small magnitudes of wavelet coefficients around these localized pulses for scales lower than 7 and higher than 8 indicate that the pulses are concentrated in the frequency range of 2.30-3.53 Hz. 2.30 Hz is the upper bound for $p = 6$, while 3.53 Hz is the lower bound for $p = 9$. For the Treasure Island vertical

wavelet coefficients, there seem to be two separated energy arrivals: one at the very beginning of the record and the other centred between 13 and 15 seconds. The one at the beginning of the record between 2 to 4 seconds has a frequency concentration between 4.60-7.06 Hz $(p = 8 \text{ and } 9)$, while the later energy arrival between 13 and 15 seconds lies in the main frequency band of 2.30-3.53 Hz $(p = 7 \text{ and } 8)$. 4.60 Hz is the upper bound of the wavelet coefficients at scale $p = 7$. The wavelet coefficients at this scale do not indicate any high peaks between 2 to 4 seconds meaning that this part of the record contains very low concentration of frequency components in the range of 0.88-4.60 Hz. As mentioned above, the wavelet coefficients were, generally, low at scale $p = 10$ or frequencies above 7.06 Hz. This clearly implies that there was a significant reduction in the frequency content of the vertical record from the start of the main motion to about 13 seconds into excitation which would indicate that the soil had considerably lost its stiffness characteristics in the vertical direction after the first few seconds of the excitation.

In contrast, the wavelet coefficients of the E-W and N-S components of Treasure Island indicate that the main energy arrival was restricted between 11 to 15 seconds and that the wavelet amplitudes have relatively small magnitudes before 11 seconds and after 15 seconds. The input energy for the E-W and N-S components of Treasure Island was mainly concentrated in the frequency range of $p = 5$ to 7 or about 0.576-1.77 Hz (for higher and lower frequency resolutions, the wavelet coefficients diminish to relatively small amplitudes). It is noted that for $p = 4$ or $0.11 < f < 0.576$ Hz, the normalized wavelet coefficients are relatively small indicating that very little energy was concentrated in the frequency range below 0.576 Hz. The wavelet peaks in this frequency range $(p = 4)$ are mainly concentrated between 15 and 25 seconds indicating a very low frequency characteristic of Treasure Island record after 15 seconds (after the occurrence of last impulse-like phase). It is noted that the frequency band of Treasure Island record after 15 seconds is mainly concentrated between 0.22-0.44 Hz. A comparison between Figures 8, 9 and 10 indicates that both the energy arrival and frequency band of wavelet coefficients for the vertical and horizontal (E-W and N-S) components of Treasure Island site are significantly different.

The WT can also provide us with further information regarding the characteristics of the last short-impulse energy arrival at Treasure Island site. Figure 9 shows that the last anomalous phase seen in the E-W record between 14 and 15 seconds has a high wavelet coefficient for $p = 5$. This indicates that the main energy of this impulse-like phase is concentrated in the frequency band of 0.576-1.15 Hz. It is noted that the wavelet amplitudes are relatively small between 14 and 15 seconds for $p = 6$ to 10. The wavelet coefficients at scales $p = 9$ and 10 represent a peak concentrated around 15 seconds indicating a significant transition in the frequency content of the signal at this time. Beyond this point, after 15 seconds, the behaviour of the signal is dominated by waves of very low-frequency content and low energy potential mainly at scales $p = 3$ and 4 in the frequency range of 0.055 - 0.44 Hz (no significant wavelet coefficient is observed between 15 to 30 seconds for frequency bands above 0.44 Hz). The spikes observed at the highest Daubechies 20-coefficient wavelet scaling parameter, $p = 10$, are representatives of abrupt changes in the frequency content of the signals. There are two distinct spikes observed at this high resolution at the Treasure Island site in both the E-W and N-S directions. The first spike in the E-W direction is seen around 13 seconds while the second spike is near the 15 seconds. In the N-S direction, the first peak is observed around 14 seconds while the second spike is located at the exact same time as in the E-W direction. The first two spikes could be interpreted as the first major change in the frequency content of the soil at the Treasure Island site which occurred with approximately 1 second time lag in the E-W and N-S directions. The second spikes, occurred at the same time in both directions, are the representatives of the most severe abrupt change in the frequency content of the signals where the overall characteristics of the soil were altered by the earthquake. At about 15 seconds into the recorded motion, the soil in Treasure Island site liquefied, which resulted in a drastic change in frequency content of the signal at this point. The fact that there is not any apparent peak at the highest resolution of the wavelets beyond 15 seconds indicates that the frequency content of the soil was not affected by the earthquake beyond this point and the change in the overall behaviour of the soil was permanent.

The reconstructed accelerations at each wavelet scale, shown in Figure 11, clearly simulate the last peak energy arrival at the Treasure Island between 13 and 15 seconds at wavelet scale $p = 5$. The reconstructed accelerations at scales $p = 7$ to 4 show a progressive drop in the frequency content of the

record from about 11 seconds to 15 seconds. This is provided by a shift to the right in the acceleration peaks at each scale.

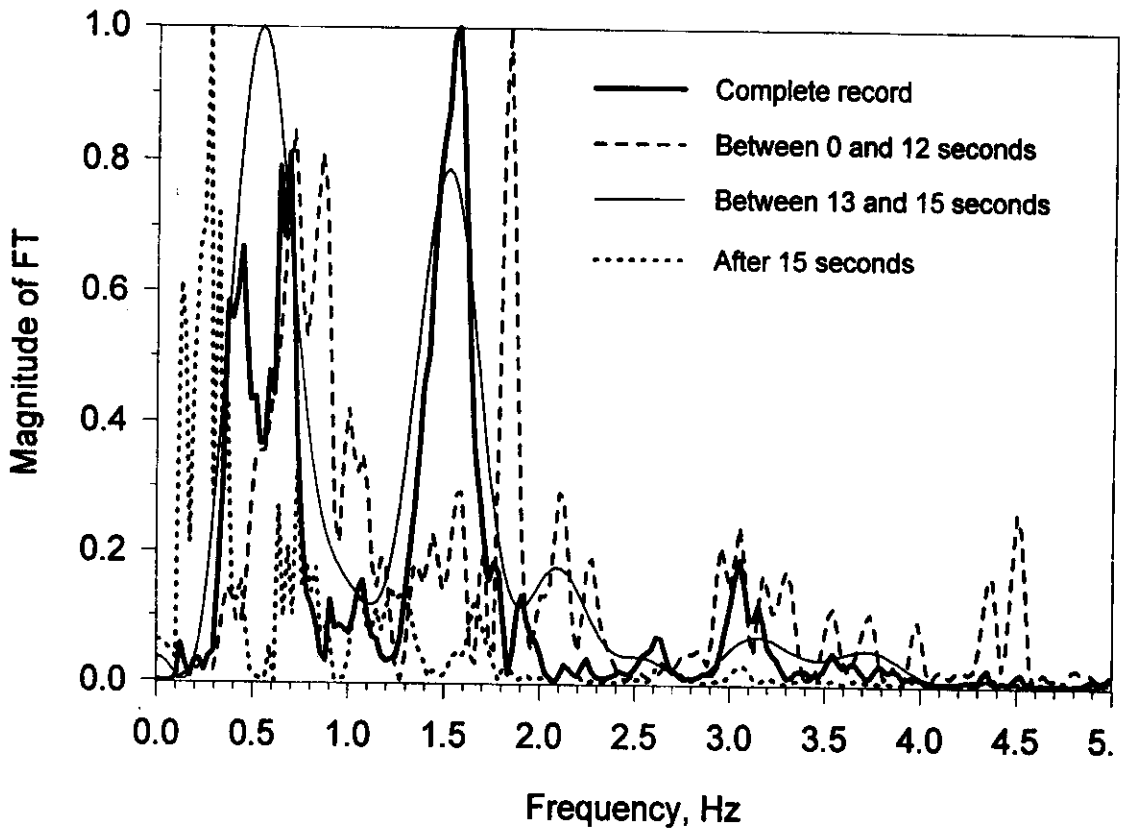

Fig. 12 Magnitude of windowed FT for the E-W component of Treasure Island

Taking into account the results of wavelet analysis, the Fourier theory was employed to study the changes in the fundamental frequency of the Treasure Island E-W acceleration component. As mentioned above, in order to have a reliable estimate of the frequency content of a signal, the effects of sudden discontinuities on the frequency domain analysis of the signals should be minimized. This could be achieved using the results from the wavelet analysis. Therefore, the peak frequencies were estimated based on the windowed FT analysis of the recorded E-W acceleration. Figure 12 shows the results of FT analysis of Treasure Island E-W acceleration record for three different window locations and for the whole record. As shown in Figure 12, for the early part of the record (between 0 and 12 seconds) the dominant frequencies are around 0.8 Hz and 1.8 Hz. As the window is placed between 13 and 15 seconds, the dominant frequencies reduce to 0.5 Hz and 1.5 Hz. After 15 seconds into the strong motion shaking, the dominant frequencies were reduced significantly to around 0.25 Hz and 0.7 Hz. This progressive reduction in the frequency content of Treasure Island E-W acceleration was also noted by the wavelet analysis. It is noted that the FT of the entire record mainly reflected the dominant frequencies between 13 and 15 seconds, as the total energy of the earthquake was significantly concentrated in this time window.

For Yerba Buena Island, the distribution of peak wavelet coefficients for the E-W component of the accelerogram, Figure 13 exhibits the main concentration of energy between 8 to 13 seconds of the record. The frequency content of the record in this interval is concentrated at scales $p = 6, 7$ and 8 between 1.15-3.53 Hz. For high wavelet scale parameters $(p = 9$ and $10)$, the peak coefficients of WT decrease to relatively small values after 15 seconds. At scale 10, however, there are some modest wavelet peaks between 11 and 15 seconds indicating the presence of abrupt changes or high frequency components in

the signal between 11 and 15 seconds; before 11 and after 15 seconds, the wavelet coefficients are relatively small.

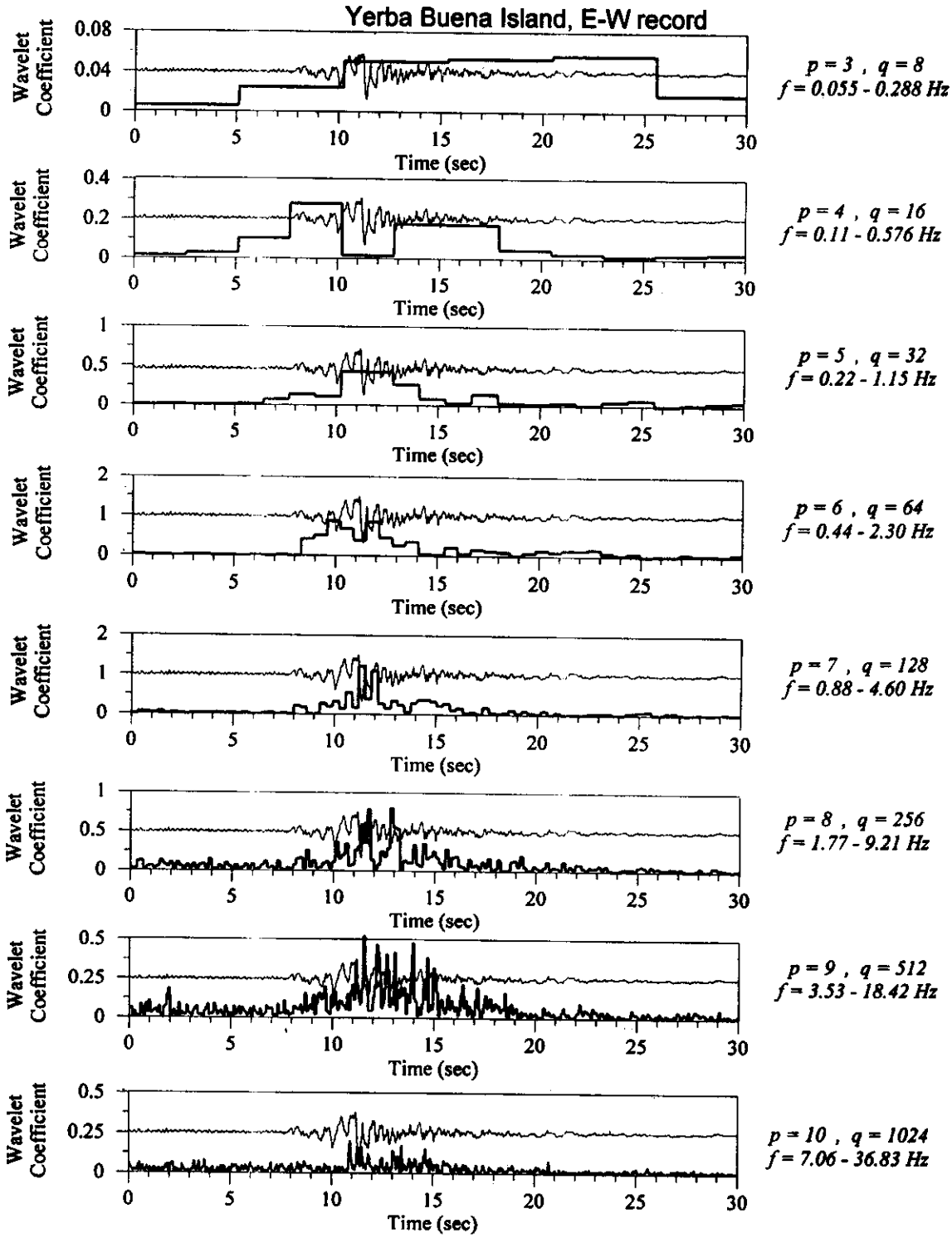

Fig. 13 Absolute magnitude of coefficients for the Daubechies 20-coefficient wavelet analysis of the Yerba Buena Island E-W acceleration, with bars at the centre of the corresponding analysing wavelet in time q for each frequency range p (thin line represents the recorded E-W acceleration for comparison purposes)

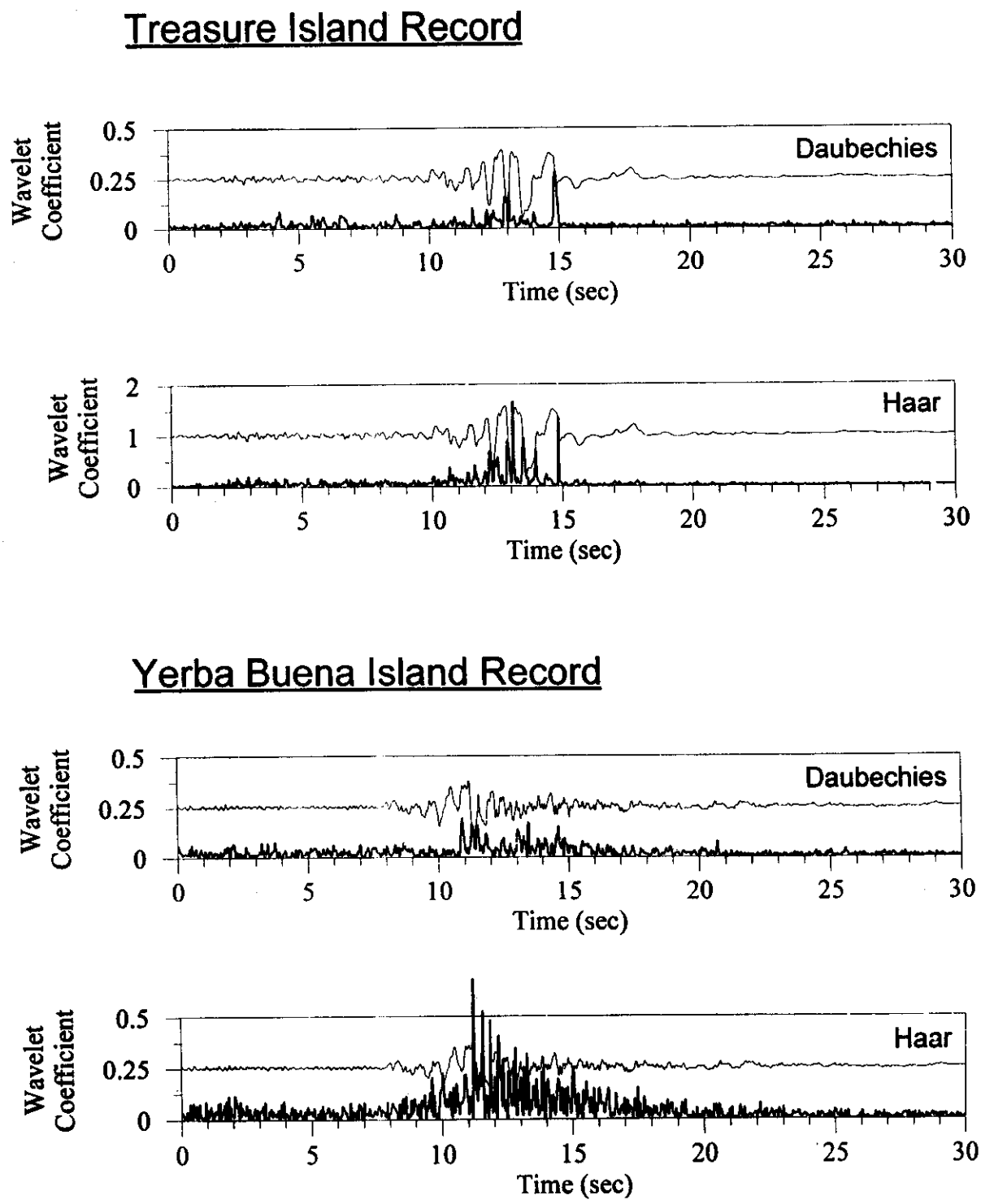

Fig. 14 Comparison of wavelet coefficients obtained using Daubechies 20-coefficient and Haar wavelets for Treasure and Yerba Buena Islands at the highest scale, $p = 9$

In order to achieve higher accuracy in determining sudden frequency shifts in the signals, both Treasure Island and Yerba Buena Island records were analysed using Haar wavelet. The results of the Haar wavelet transform for both records at the finest scale, $p = 10$, in comparison with Daubechies 20-coefficient wavelet transform are shown in Figure 14. There are some noticeable peaks at this scale in Treasure Island and Yerba Buena Island records. The Haar wavelet is more sensitive in detecting the variation of frequency content of the signals as we observe more pronounced spikes (larger wavelet coefficients) in both records. Most of the wavelet peaks have similar temporal domains for both Daubechies 20-coefficient and Haar wavelets. Similar to the results from the Daubechies 20-coefficient wavelet analysis, the one last large peak in the Treasure Island record near 15 seconds could be attributed to the major transition in the frequency content of the signal when the soil underwent a drastic change. At about 15 seconds into the recorded motion, the soil in Treasure Island site liquefied, which resulted in a severe change in the frequency content of the signal at this point with no other changes beyond this point.

CONCLUSIONS

Wavelet transforms can be very useful to identify any phases in a signal which are localized in both time and frequency. The present wavelet analysis reveals the properties of an anomalous impulse-like late energy phase in Treasure Island accelerogram. The phase is found to be between 13 and 15 seconds, and with a frequency range of 0.22-0.44 Hz. The orthonormal wavelet coefficients also give information about sudden frequency changes in the records. In this case, it has been possible to identify anomalies in the records associated with soil liquefaction by analysing the two records and detecting the change in the dynamic behaviour of signals which occur when there is an abrupt change in the frequency. Considering the time lag between the two records, some of the peaks are associated with the inherent abrupt changes in the frequency content of ground motion. The one peak at 15 seconds, however, could be attributed to the most abrupt change in the frequency content of the Treasure Island signal.

Since there are rapid developments being made in studies of wavelet transforms, the present Daubechies 20-coefficient or Haar wavelets are not the ultimate tools to establish time-scale planes for seismological data. The Haar wavelet is usually more suitable for detecting edges in a signal. The use of an appropriate analysing wavelet for seismic data is a key to making data analysis successful. The present wavelet transforms demonstrate a great potential for the study of interesting features hidden in strong motion data.

ACKNOWLEDGEMENTS

Funding for this study was provided by a research grant from the Natural Sciences and Engineering Research Council of Canada (NSERC). Valuable discussions with Jahan Ghofraniha of the Department of Electrical Engineering at the University of British Columbia during the course of study of wavelet transforms are acknowledged with thanks.

REFERENCES

1. Daubechies, I. (1988). "Orthonormal Bases of Compactly Supported Wavelets", Comm. on Pure and Appl. Math., Vol. 4, pp. 909-996.
2. Daubechies, I. (1992). "Ten Lectures on Wavelets", Society for Industrial and Applied Mathematics, Philadelphia, U.S.A.
3. Finn, W.D.L., Ventura, C.E. and Wu, G. (1993). "Analysis of Ground Motions at Treasure Island Site during the 1989 Loma Prieta Earthquake", Soil Dynamics and Earthquake Engineering, Vol. 12, No. 7, pp. 383-390.
4. Gabor, D. (1946). "Theory of Communication", Journal of Inst. Elec. Eng., Vol. 93, pp. 429-457.
5. Grossmann, A. and Morlet, J. (1984). "Decomposition of Hardy Functions into Square Integrable Wavelets of Constant Shape", SIAM J. Math. Anal., Vol. 15, pp. 723-736.
6. Kronland-Martinet, R., Morlet, J. and Grossmann, A. (1987). "Analysis of Sound Patterns through Wavelet Transforms", International Journal of Pattern Recognition and Artificial Intelligence, Vol. 1, No. 2, pp. 97-125.

7. Mallat, S.G. (1989). "A Theory for Multiresolution Signal Decomposition: The Wavelet Representation", IEEE Trans. on Pattern Anal. and Machine Intel., Vol. 11, pp. 674-693.
8. Mallat, S.G. (1989). "Multifrequency Channel Decompositions of Images and Wavelet Models", IEEE Transactions on Acoustics, Speech and Signal Processing, Vol. 37, No. 12, pp. 2091-2110.
9. Meyer, Y. (1986). "Ondelettes et Fonctions Splines Seminaire EDP", Ecole Polytechnique, Paris, France.
10. Newland, D.E. (1993). "Random Vibrations, Spectral and Wavelet Analysis", 3rd Edition, Longman, Harlow, U.K.
11. Rioul, O. and Vetterli, M. (1991). "Wavelets and Signal Processing", IEEE Signal Processing Magazine, pp. 14-38.
12. Shakal, A., Huang, M., Reichle, M., Ventura, C.E., Cao, T., Sherburne, R., Savage, M., Darragh, R. and Petersen, C. (1989). "CSMIP Strong Motion Records from the Santa Cruz Mountains (Loma Prieta), California Earthquake of 17 October 1989", California Department of Conservation, Division of Mines and Geology, Office of Strong Motion Studies, U.S.A.
13. Strang, G. (1989). "Wavelets and Dilation Equations: A Brief Introduction", SIAM Review, Vol. 31, No. 4, pp. 614-627.
14. Vetterli, M. and Herley, C. (1992). "Wavelets and Filter Banks: Theory and Design", IEEE Transactions on Signal Processing, Vol. 40, No. 9, pp. 2207-2232.